Mendeleev Communications

Mendeleev Commun., 2025, **35**, 684–687

Lateral photoresistor as a versatile device platform for stability assessment of organic semiconductors

Petr M. Kuznetsov,[a] Sergey L. Nikitenko,[a] Mikhail V. Zhidkov,[a] Dmitry P. Kirukhin,[a] Evgeniy V. Golosov[a] and Pavel A. Troshin*[b,a]

[a] *Federal Research Center of Problems of Chemical Physics and Medicinal Chemistry, Russian Academy of Sciences, 142432 Chernogolovka, Moscow Region, Russian Federation. E-mail: troshin2003@inbox.ru*
[b] *Zhengzhou Research Institute, Harbin Institute of Technology, 450003 Zhengzhou, China*

DOI: 10.71267/mencom.7711

We address the challenge of the reliable stability assessment of organic semiconductors and propose a solution based on the application of a very simple lateral photoresistor device structure as a versatile test platform. The device, which consists of the semiconductor films deposited on the laser-patterned electrodes, could be exposed to different stress factors, and the evolution of the electrical characteristics of the active material (basically, its ability to transport charges) can be monitored using current–voltage measurements under steady-state or dynamic light exposure. This approach has been successfully applied to evaluate the radiation hardness and the UV light photostability of a model set of conjugated polymers.

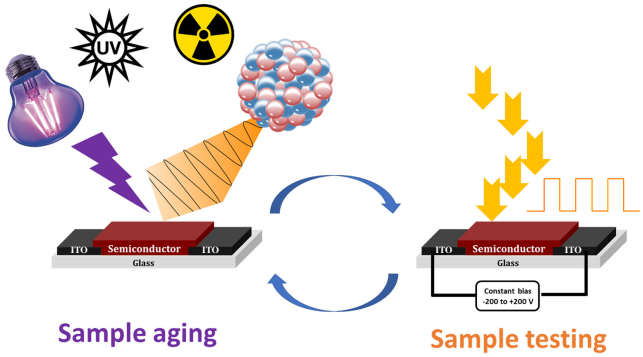

Keywords: organic semiconductors, organic electronics, stability, photostability, radiation hardness.

Organic electronics is rapidly developing nowadays and represents a highly promising technology with many commercialized products.[1,2] This includes organic field-effect transistors (OFETs) and electronic circuits,[3,4] electronic textiles,[5,6] organic solar cells,[7] organic light-emitting diodes and the associated mainstream technology of OLED displays,[8] bioelectronics,[9] different types of wearable sensors,[10,11] and even artificial retinas.[12–14] All these exciting applications rely on specific organic semiconductors with tailorable optoelectronic and physicochemical properties.[15] The closer we come to the commercial products based on organic electronics, the more important the enhancement of the operational stability of the corresponding devices and, hence, the intrinsic stability of the used semiconductor materials becomes.[16,17] This problem is quite severe for organic solar cells,[18,19] blue OLEDs,[20] OFETs,[21] sensor platforms[22] and basically all other components.

Therefore, some simple testing platform relevant to the material operation regime in the final device has to be developed. Herein, we address this challenge and present the lateral photoresistor device geometry [Figure 1(*a*)] as a universal solution for the stability assessment of organic semiconductors under exposure to UV light, ionizing radiation, and potentially many other stress factors.

We have been long pursuing the problem of the investigation of intrinsic photostability of organic and hybrid semiconductors, which is important for stability enhancement in organic solar cells.[23–28] In that context, we were seeking a device architecture that should satisfy three basic requirements: (1) the device degradation must be directly related to the semiconductor material degradation; (2) the device degradation must be the least dependent on the electrode/material interface behavior; and (3) tested material should be exposed on the surface for direct contact with the stress factor, such as, *e.g.*, UV light. As an illustration, bottom-gate top-contact OFET geometry would not satisfy these criteria since the electrical characteristics of such a device depend mostly on the interface between the semiconductor and dielectric and are also strongly affected by the behavior of the top contacts, *e.g.*, metal ion diffusion. Vertical two-electrode device geometry would not also be appropriate since the device

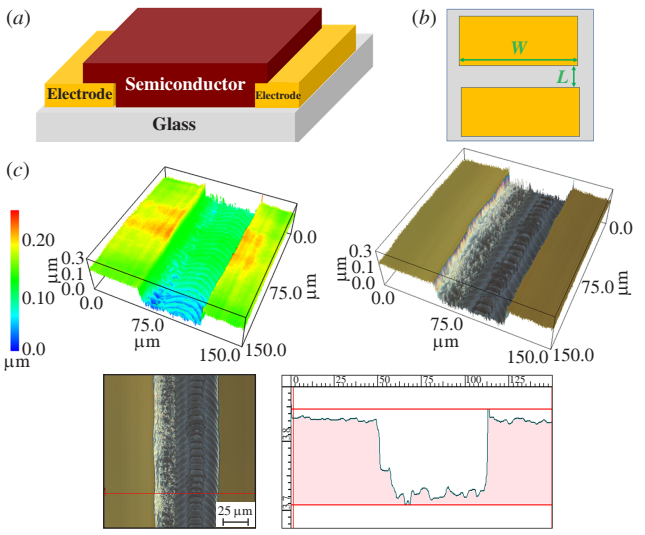

Figure 1 (*a*) Layout of the lateral photoresistor device geometry and (*b*) the schematic top-view representation showing the channel dimensions. (*c*) 3D and 2D microscopy visualization of the channel produced in the ITO electrode by YAG (1064 nm) laser scribing.

degradation mostly depends on the top (and sometimes also bottom) electrode material diffusion into the semiconductor, whereas the tested material is not accessible, *e.g.*, for UV light, since even the transparent metal oxide electrodes are blocking UV photons.

In view of these considerations, we proposed to use lateral photoresistor device geometry for *in situ* or even *operando* assessment of the electrical properties of the organic semiconductor material during aging under exposure to different stress factors. It is of notice, however, that such device geometry could be sensitive to the extrinsic stress factors (*e.g.*, oxygen or moisture), so all the experiments have to be performed in the well-controlled environment or using some appropriate encapsulation.

The device fabrication starts from the evaporation of a metal film (usually gold) on the pre-cleaned glass substrates or using commercial glass with the conductive indium tin oxide (ITO) layer. Afterwards, the conductive layer of Au or ITO is patterned by the laser scribing process to produce the desired electrode geometry. In the simplest case, the electrodes can be rectangular-shaped, as shown in [Figure 1(*a*),(*b*)], with the well-defined channel length (in our case, $L = 50–70$ μm) and width ($W = 2$ mm). However, the interdigitated 'finger-type' geometry can also be realized in order to increase the formal channel width and the total current flowing through the channel during the device operation. We found patterned ITO the most convenient and reliable electrode platform for the investigation of organic semiconductors, even though gold electrodes may be more chemically inert with respect to organic materials. However, some chelation-type interactions of gold with organic semiconductors or even gold dissolution cannot be excluded.[29] The standard ITO scribing process with the YAG laser (1064 nm) can produce the 50–70 μm wide channels as shown in Figure 1(*c*), whereas the application of the UV laser (355 nm) under the optimized scribing conditions could produce the channels narrower than 20 μm (see Online Supplementary Materials, Figure S1). After the laser patterning, the electrodes are washed again, dried, and then thin films of organic semiconductors are spin-coated on top in inert atmosphere inside a nitrogen-filled glove box to avoid material contamination and any kind of ambient degradation.

Herein, we assessed the photostability of a series of conjugated polymers **P1**–**P15** with diketo pyrrolopyrrole units, which we studied in detail using UV-VIS and PL spectroscopy previously.[38] Samples **P3HT** and **PCDTBT** were used as the reference benchmarks (Figure 2).

The electrical characteristics of the fabricated devices were first measured by sweeping the voltage applied to the two device terminals from –200 to 200 V in the dark. Due to the high resistance of the polymer films, the maximum dark currents were in the range of 10–100 pA for pristine (non-aged) samples. Such low current values challenged the investigation of the device aging behavior since the conductivity of the materials is expected to decay upon aging. However, the same devices exhibited a few orders of magnitude higher currents under exposure to the light provided by a 10 W white light-emitting diode due to the well-known photoconductivity effect in organic semiconductors. Therefore, we could follow the evolution of the current–voltage (*I*–*V*) characteristics of the devices upon aging under exposure to the hard UV light illumination (mercury lamp, 254 nm, ~30 mW cm^{-2}). The overall scheme of the

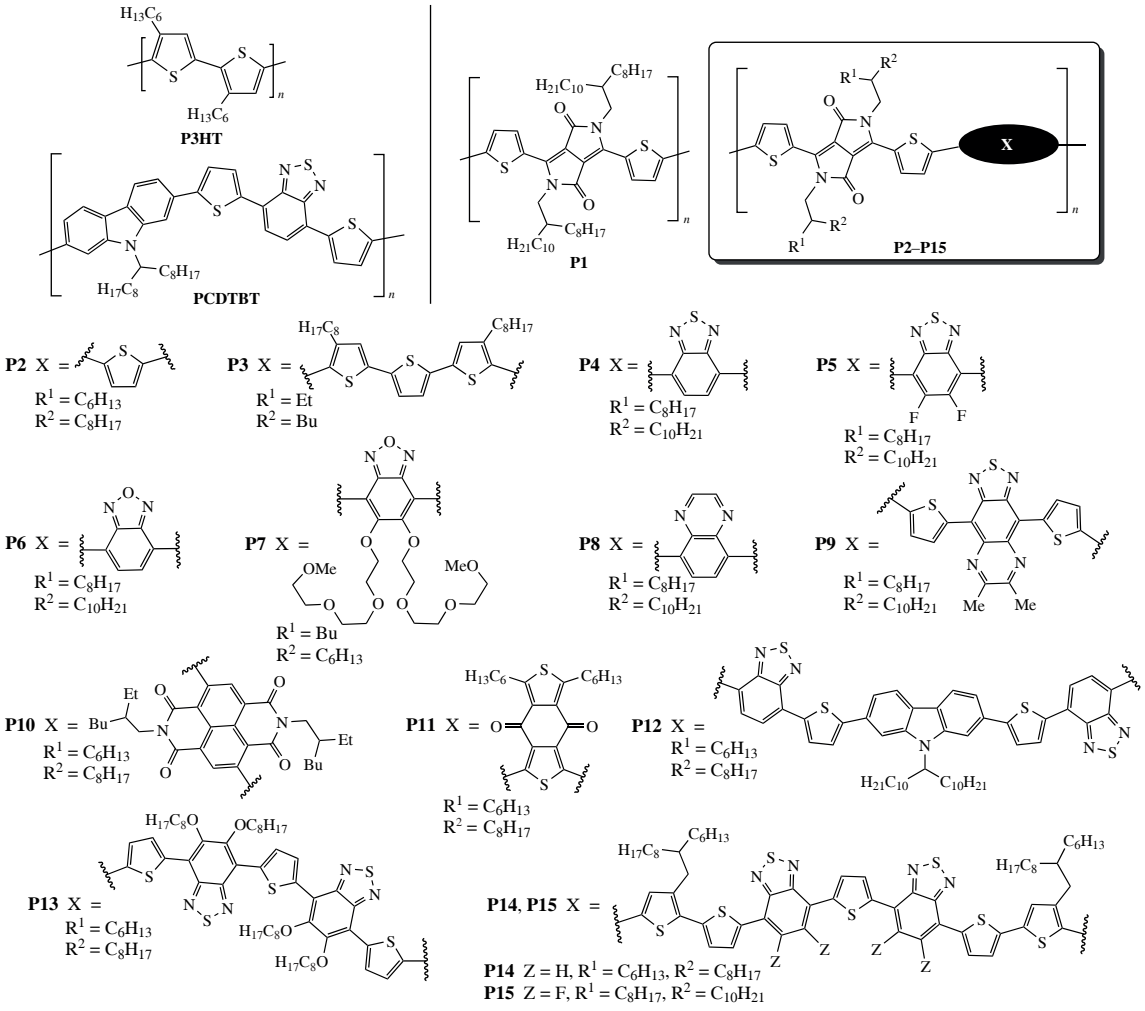

Figure 2 Molecular structures of the studied polymers **P1**–**P15**, **P3HT**, and **PCDTBT**.

experiment is featured in Figure 3(*a*): basically, the samples were repeatedly flipped between the UV aging (or gamma rays aging) chamber and the measurement station, so each device generated a set of electrical characteristics evolving with the aging time.

It has been observed that the maximum current transported through the channel of the devices was rapidly decaying upon an increase in the UV light exposure time [Figure 3(*b*)]. This kind of behavior is expectable since UV light breaks down the conjugated bond system in the polymer backbone, which results in deterioration of their semiconductor characteristics. In addition to the steady-state measurements, valuable information could be obtained from the transient photoresponse profiles to a series of relatively long (5 s) light pulses. The magnitude of the photoresponse signal is rapidly decaying after UV aging, which confirms the degradation of the material characteristics. It should also be noticed that UV light aging affects the shape of the photoresponse signal: the rise and decay fronts become less steep after short UV exposure (*e.g.*, 0.5 h), which suggests the accumulation of charge carriers in the photogenerated traps in the device channel. However, severe degradation of the material results in the opposite behavior, so the rise of the photoresponse becomes steeper after 2.5 h of aging. Similar behavior was observed for all studied materials. Therefore, it seems that additional information, *e.g.*, characteristic time constants, could be extracted from the obtained data after appropriate models and analysis are introduced.

The same technique could also be applied to assess the radiation hardness of organic semiconductors. Using devices with two model polymers, **P3HT** and **PCDTBT**, we demonstrate that the amplitude of their photoresponse is gradually decreasing after exposure to different doses of ^{60}Co gamma rays [see Figure 3(*e*),(*f*)]. It should be emphasized that both polymers maintain their semiconductor properties even after exposure to the ultrahigh doses of 2 MGy, which makes a sharp contrast to conventional inorganic semiconductors (*e.g.*, silicon) that are much more sensitive to the ionizing radiation. The obtained results feature the potential of organic semiconductors in the development of radiation-tolerant electronics.

Using the developed approach, we compared the UV light hardness of the studied conjugated polymers **P1**–**P15**, **P3HT** and **PCDTBT**. Figure 4(*a*) shows the evolution of the photoresponse amplitude for the corresponding devices plotted as a function of the aging time. By comparing the time dynamics of the photoresponse, we can benchmark the photostability of the tested active conjugated polymers (part *b*). One could notice that devices comprised of **PCDTBT** thin films show very stable operational behavior. However, the same or even better stability has been demonstrated by conjugated polymers **P13**–**P15**, all possessing extended **TBTBT** blocks composed of alternating thiophene and benzothiadiazole units. Polymers **P2**, **P3**, and **P10** demonstrated comparably good stability matching that of the reference material **P3HT**. It is notable that **P2** and **P3** incorporate thiophene and terthiophene X blocks in the molecular structure, while **P10** is loaded with a naphthalenediimide fragment, which is well-known for its excellent stability. However, the lowest stability was demonstrated by polymers **P4**–**P6**, which have electron-deficient benzothiadiazole and benzoxadiazole X units, as well as homopolymer **P1**. The obtained results suggest that for achieving stable electrical performance of conjugated polymers under UV light exposure, the parent diketo pyrrolopyrrole block should be combined with the electron-rich (*e.g.*, thiophenes in **P2**–**P3**) or extended donor–acceptor push–pull (**P13**–**P15**) conjugated systems. On the contrary, combining this block with other electron-deficient units yields materials with low stability, with the only exception being **P10**, which is stabilized by the extended naphthalenediimide framework. It should be emphasized that the revealed polymer structure–device stability

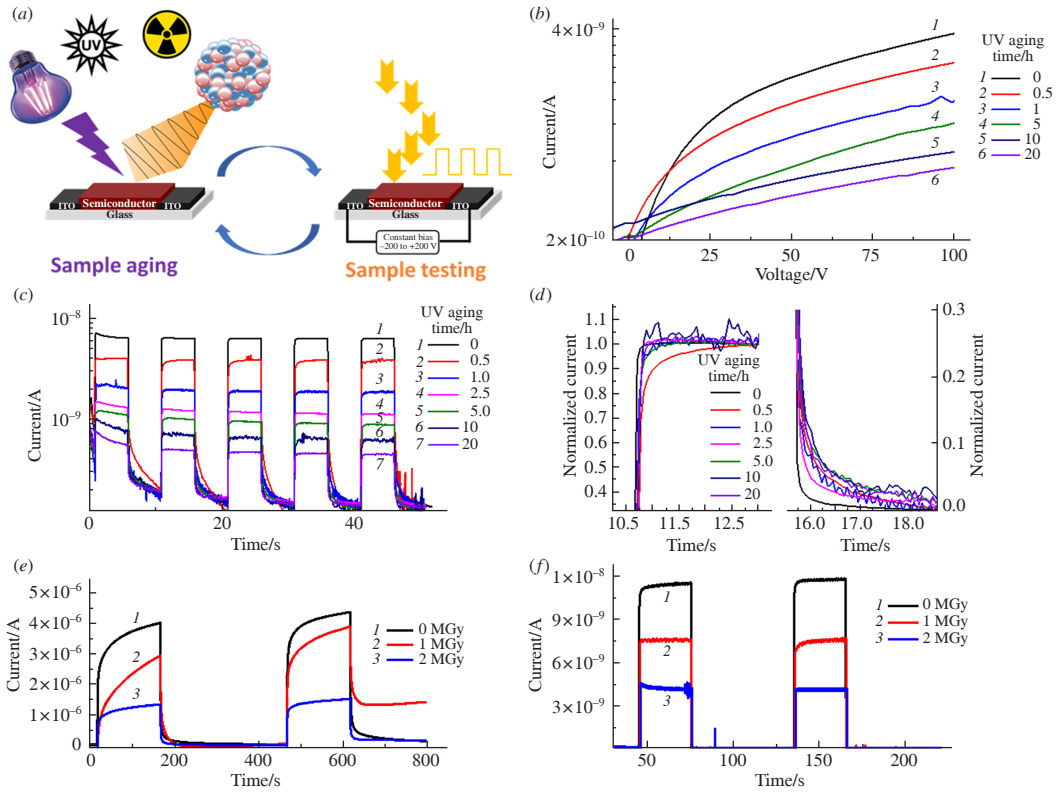

Figure 3 (*a*) The schematic layout of the experiment with the loop of the sample aging and characterization sessions. (*b*) The evolution of the *I*–*V* characteristics of the device based on **P8** as a function of the UV aging time. (*c*) The change in the dynamic photoresponse of the device based on the same material to a series of 5 s light pulses under the constant bias of 200 V. (*d*) The zoomed signal rise and decay regions of the normalized photoresponse show the effect of the aging on the corresponding time constants. (*e*), (*f*) The evolution of the dynamic photoresponse of the devices with thin films of **P3HT** (*e*) and **PCDTBT** (*f*) upon exposure to different doses of gamma rays.

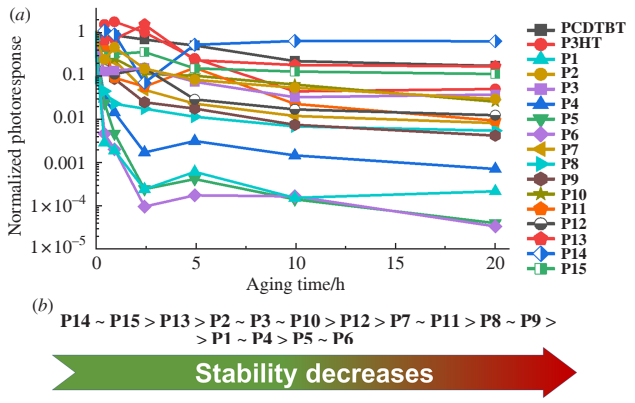

Figure 4 (*a*) The evolution of the normalized photoresponse of the devices based on different polymer films as a function of the UV exposure time. (*b*) Benchmarking conjugated polymers **P1**–**P15** in terms of the stability of their electrical properties under UV light exposure.

relationships are quite different from the correlations built based on the optical UV-VIS and PL spectroscopy for the same group of polymers.[38] This finding confirms our hypothesis that a similar evolution of optical properties of structurally distinct organic semiconductor materials under UV light exposure can cause dramatically different effects on their electrical properties. Basically, this could be explained by different depths of traps for charge carriers generated in different polymer structures under the UV light exposure. Therefore, the proposed in this work methodology to monitor the evolution of the electrical properties of organic semiconductor films under UV light or radiation exposure appears to be highly relevant to the target application of these materials.

In conclusion, we utilized a lateral photoresistor device architecture as a simple and highly reliable test platform for rapid stability assessment of organic semiconductors with respect to different stress factors. In addition to the UV light and gamma rays used in this work, the proposed approach can be potentially useful to study the effects of any type of ionizing radiation, visible light, heat, ambient species, *etc*., on the electrical performance of organic semiconductors. The developed technique relies on the deterioration of the charge transport properties of the semiconductor materials upon aging, which is their basic functionality utilized in practically useful devices. Therefore, we believe that the approach presented here provides more adequate and trustworthy stability assessment of organic semiconductor materials than the alternative approaches based on different spectroscopy techniques.

This work was supported by The Russian Science Foundation (grant no. 22-43-04427). Authors gratefully acknowledge the participation of Dr. A. V. Akkuratov, Dr. I. E. Kuznetsov in the synthesis of some of the studied conjugated polymers and Dr. I. V. Martynov for preparation of samples for the radiation exposure tests.

Online Supplementary Materials

Supplementary data associated with this article can be found in the online version at doi: 10.71267/mencom.7711.

References

1 M. Catacchio, M. Caputo, L. Sarcina, C. Scandurra, A. Tricase, V. Marchianò, E. Macchia, P. Bollella and L. Torsi, *Faraday Discuss.*, 2024, **250**, 9; https://doi.org/10.1039/D3FD00152K.
2 W. Fan, *Nat. Mater.*, 2023, **22**, 1274; https://doi.org/10.1038/s41563-023-01681-3.
3 K. Tie, J. Qi, Y. Hu, Y. Fu, S. Sun, Y. Wang, Y. Huang, Z. Wang, L. Yuan, L. Li, D. Wei, X. Chen and W. Hu, *Sci. Adv.*, 2024, **10**, eadn5964; https://doi.org/10.1126/sciadv.adn5964.
4 S. Park, S. H. Kim, H. Lee and K. Cho, *npj Flex. Electron.*, 2024, **8**, 71; https://doi.org/10.1038/s41528-024-00359-3.
5 H. T. H. Shi, Y. Pan, L. Xu, X. Feng, W. Wang, P. Potluri, L. Hu, T. Hasan and Y. Y. S. Huang, *Nat. Mater.*, 2023, **22**, 1294; https://doi.org/10.1038/s41563-023-01615-z.
6 I. McCulloch, M. Chabinyc, C. Brabec, C. B. Nielsen and S. E. Watkins, *Nat. Mater.*, 2023, **22**, 1304; https://doi.org/10.1038/s41563-023-01579-0.
7 P. Ding, D. Yang, S. Yang and Z. Ge, *Chem. Soc. Rev.*, 2024, **53**, 2350; https://doi.org/10.1039/D3CS00492A.
8 H. Wang, Y. Yuan, Z. S. Wang and Y. Wang, *ACS Appl. Eng. Mater.*, 2024, **2**, 781; https://doi.org/10.1021/acsaenm.4c00196.
9 W. Wang, Y. Pan, Y. Shui, T. Hasan, I. M. Lei, S. G. S. Ka, T. Savin, S. Velasco-Bosom, Y. Cao, S. B. P. McLaren, Y. Cao, F. Xiong, G. G. Malliaras and Y. Y. S. Huang, *Nat. Electron.*, 2024, **7**, 586; https://doi.org/10.1038/s41928-024-01174-4.
10 B. King and B. H. Lessard, *J. Mater. Chem. C*, 2024, **12**, 5654; https://doi.org/10.1039/D3TC03611A.
11 D. S. Anisimov, V. P. Chekusova, A. A. Trul, A. A. Abramov, O. V. Borshchev, E. V. Agina and S. A. Ponomarenko, *Sci. Rep.*, 2021, **11**, 10683; https://doi.org/10.1038/s41598-021-88569-x.
12 L. Torsi, M. Magliulo, K. Manoli and G. Palazzo, *Chem. Soc. Rev.*, 2013, **42**, 8612; https://doi.org/10.1039/c3cs60127g.
13 J. F. Maya-Vetencourt, D. Ghezzi, M. R. Antognazza, E. Colombo, M. Mete, P. Feyen, A. Desii, A. Buschiazzo, M. Di Paolo, S. Di Marco, F. Ticconi, L. Emionite, D. Shmal, C. Marini, I. Donelli, G. Freddi, R. Maccarone, S. Bisti, G. Sambuceti, G. Pertile, G. Lanzani and F. Benfenati, *Nat. Mater.*, 2017, **16**, 681; https://doi.org/10.1038/nmat4874.
14 S. Wang, X. Shi, J. Gong, W. Liu, C. Jin, J. Sun, Y. Peng and J. Yang, *Nano Lett.*, 2024, **24**, 3204; https://doi.org/10.1021/acs.nanolett.4c00087.
15 Q. Zhang, W. Hu, H. Sirringhaus and K. Müllen, *Adv. Mater.*, 2022, **34**, 2108701; https://doi.org/10.1002/adma.202108701.
16 L. Yao, N. Guijarro, F. Boudoire, Y. Liu, A. Rahmanudin, R. A. Wells, A. Sekar, H.-H. Cho, J.-H. Yum, F. Le Formal and K. Sivula, *J. Am. Chem. Soc.*, 2020, **142**, 7795; https://doi.org/10.1021/jacs.0c00126.
17 C. G. Tang, K. Hou and W. L. Leong, *Chem. Mater.*, 2024, **36**, 28; https://doi.org/10.1021/acs.chemmater.3c02093.
18 N. A. Tegegne, L. T. Nchinda and T. P. J. Krüger, *Adv. Opt. Mater.*, 2025, **13**, 2402257; https://doi.org/10.1002/adom.202402257.
19 M. Wu, B. Ma, S. Li, J. Han and W. Zhao, *Adv. Funct. Mater*., 2023, **33**, 2305445; https://doi.org/10.1002/adfm.202305445.
20 E. Tankelevičiūtė, I. D. W. Samuel and E. Zysman-Colman, *J. Phys. Chem. Lett.*, 2024, **15**, 1034; https://doi.org/10.1021/acs.jpclett.3c03317.
21 K. Sakamoto, T. Yasuda, T. Minari, M. Yoshio, J. Kuwabara and M. Takeuchi, *ACS Appl. Mater. Interfaces*, 2024, **16**, 68081; https://doi.org/10.1021/acsami.4c15666.
22 L. Luo and Z. Liu, *VIEW*, 2022, **3**, 20200115; https://doi.org/10.1002/VIW.20200115.
23 P. M. Kuznetsov, E. A. Komissarova, S. A. Kuklin and P. A. Troshin, *Mendeleev Commun.*, 2024, **34**, 338; https://doi.org/10.1016/j.mencom.2024.04.009.
24 P. M. Kuznetsov, I. V. Martynov, I. S. Zhidkov, L. G. Gutsev, E. A. Komissarova, A. V. Maskaev, A. I. Kukharenko, F. A. Prudnov and P. A. Troshin, *J. Phys. Chem. B*, 2023, **127**, 6432; https://doi.org/10.1021/acs.jpcb.3c03242.
25 P. M. Kuznetsov, I. V. Martynov, I. S. Zhidkov, L. G. Gutsev, E. A. Khakina, E. N. Zakharchenko, N. A. Slesarenko, A. I. Kukharenko and P. A. Troshin, *J. Mater. Chem. A*, 2023, **11**, 9019; https://doi.org/10.1039/D2TA09402A.
26 P. A. Troshin, D. K. Susarova, Y. L. Moskvin, I. E. Kuznetsov, S. A. Ponomarenko, E. N. Myshkovskaya, K. A. Zakharcheva, A. A. Balakai, S. D. Babenko and V. F. Razumov, *Adv. Funct. Mater*., 2010, **20**, 4351; https://doi.org/10.1002/adfm.201001308.
27 L. A. Frolova, N. P. Piven, D. K. Susarova, A. V. Akkuratov, S. D. Babenko and P. A. Troshin, *Chem. Commun.*, 2015, **51**, 2242; https://doi.org/10.1039/C4CC08146C.
28 O. R. Yamilova, I. V. Martynov, A. S. Brandvold, I. V. Klimovich, A. H. Balzer, A. V. Akkuratov, I. E. Kusnetsov, N. Stingelin and P. A. Troshin, *Adv. Energy Mater*., 2020, **10**, 1903163; https://doi.org/10.1002/aenm.201903163.
29 G. Ligorio, M. V. Nardi, C. Christodoulou and N. Koch, *ChemPhysChem*, 2015, **16**, 2602; https://doi.org/10.1002/cphc.201500337.

Received: 13th December 2024; Com. 24/7711